Available online at www.sciencedirect.com

SciVerse ScienceDirect

Journal of the European Ceramic Society 32 (2012) 1965–1970

www.elsevier.com/locate/jeurceramsoc

The influence of additives on microstrucutre of sub-micron alumina ceramics prepared by two-stage sintering

Dušan Galusek [a,*], Katarína Ghillányová [b], Jaroslav Sedláček [a], Jana Kozánková [c], Pavol Šajgalík [b]

[a] *Vitrum Laugaricio – Joint Glass Centre of the IIC SAS, TnU AD, FChPT STU and RONA, a.s., Študentská 2, SK-911 50 Trenčín, Slovak Republic*
[b] *Institute of Inorganic Chemistry, Slovak Academy of Sciences, Dúbravská cesta 9, SK-845 36 Bratislava 45, Slovak Republic*
[c] *Faculty of Chemical and Food Technology, Slovak Technical University, Radlinského 9, SK-812 37 Bratislava, Slovak Republic*

Available online 19 December 2011

Abstract

For various systems two-stage sintering has been reported as a successful way of suppressing the grain growth in the final stage of densification of polycrystalline ceramics. Our previous results on two-stage sintering of high purity submicrometre polycrystalline alumina indicate limited efficiency of the process with respect to suppression of grain growth. The present work deals with the influence of deliberate additions of various metal oxides (500 ppm of MgO, Y_2O_3 or ZrO_2) whose grain growth retarding effect in conventional sintering has been well documented, on two-stage sintering of submicrometre alumina ceramics. The addition of MgO was observed to enhance densification. Addition of yttria and zirconia impaired densification, but addition of all three dopants resulted in suppression of the grain growth and microstructure refinement in comparison to undoped alumina.

Keyword: Alumina ceramics; Sintering; Grain size; Grain growth; Microstructure-final

1. Introduction

The sintering of advanced ceramics is often conducted in the way, which ensures high final density of prepared material with homogeneous microstructure consisting of small grains. This type of microstructure is associated with better mechanical properties, especially hardness, bending strength and wear resistance, compared to their coarse grained counterparts. One of the ways of elimination of grain growth in the final stage of sintering is two-stage sintering process reported by Chen and Wang.[1] This was originally successfully applied for densification of a nanometer-sized yttria powder without the final stage grain growth. The authors postulated that at a certain temperature interval called "kinetic window" densification is already in operation, whilst the grain boundary motion is not yet activated. Sintering in this temperature region then results in elimination of residual porosity without the final stage grain growth. The method has been successfully applied for sintering of Ni–Cu–Zn ferrite, barium titanate[2,3] zirconia,[4] and a range of other materials.[5–8] Although the two-stage sintering applied to pure alumina showed certain refinement of microstructure in comparison to conventional sintering, the grain growth in the final stage of densification was not entirely suppressed.[9–11] Full applicability of the two-stage sintering for pure alumina is therefore rather questionable: the results of Kanters et al. even suggest that the activation energy of densification in alumina is higher than the activation energy of grain growth.[12] If true, the "kinetic window" cannot exist, and no temperature interval can be found, where complete densification of alumina without the final stage grain growth can be achieved.

The addition of various metal oxides at ppm level is known to alter the behaviour during the solid state sintering of alumina, through influencing both the grain mobility and the rate of densification. Associated change of activation energy of either process offers new possibilities for successful application of solid state two-stage sintering of alumina.

Although the exact mechanism of its action is still the matter of much controversy, the most frequently used and most efficient grain growth suppressor is considered MgO, and for many years a small addition of MgO has been a key processing step for suppression of abnormal grain growth in alumina. Many studies attempted to explain the mechanism of action of MgO, both for

* Corresponding author. Tel.: +421 32 7400590.
E-mail address: dusan.galusek@tnuni.sk (D. Galusek).

0955-2219/$ – see front matter © 2011 Elsevier Ltd. All rights reserved.
doi:10.1016/j.jeurceramsoc.2011.11.038

solid and liquid phase sintering of alumina. The proposed mechanisms for solid state sintering include solute drag,[13] and the change of interface structure from atomically smooth to atomically rough with corresponding increase of surface and grain boundary diffusion.[14] According to the solute drag (or pinning) model, the major role of MgO is reduction of the grain boundary mobility as a solute in the corundum crystal or segregated preferentially in the grain boundaries. The model was created on the basis of experimental observation that the rate of grain growth in dense high purity alumina was reduced significantly with MgO doping by annealing at 1600 °C.[13]

According to Jo et al.[14] the role of MgO may be attributed to the change in interface structure of alumina grains. It was observed that atomically smooth surface of alumina became atomically rough when heat treated in MgO-containing atmosphere. Then the grain growth is not controlled by interface reaction, but by diffusion, and the number of grains that can grow increases to such extent that they impinge each other and abnormal grain growth does not occur. Except of promoting grain growth the roughening of atomically smooth surfaces explains also the enhanced densification rate, as diffusion in the system with disordered grain boundaries is expected to be easier. Berry and Harmer[15] reasoned the densification increases through an increase of the diffusion rate and the enhanced grain growth explained by an increase of the surface diffusion coefficient. Small-angle neutron scattering measurements indicated that the role of MgO as a sintering aid lies, at least in part, in prolonging the stability of intermediate stage of sintering such that the body achieves greater density before the transition to final-stage sintering, after which isolated pores are formed.[16]

Another group of dopants is represented by metal oxides, which strongly segregate at alumina–alumina interfaces, such as yttria and zirconia. Due to its limited solubility in alumina crystal lattice (∼10 atomic ppm) yttrium segregates to α-alumina surfaces,[17,18] and improves the creep resistance at high temperatures.[19,20] This makes yttria a common dopant in many applications. Yttria doping was found to inhibit both densification and grain growth of alumina but the effect is much reduced with increasing temperature. This behaviour may be related to a transition with increasing temperature from grain boundary diffusion to lattice diffusion controlled densification.[21,22] Similar effect on creep was observed also by minor ZrO_2 addition, which similarly to yttria, also hinders the grain growth of Al_2O_3.[23]

Present work investigates the influence of dopants known to influence densification and grain growth during conventional sintering under the conditions of two stage sintering regime. Both the additives, which are known to enhance the grain growth and densification, such as MgO, and those which are known as densification and grain growth inhibitors (Y_2O_3 and ZrO_2) are applied, and their influence on the final stage grain growth is studied and discussed.

2. Experimental

High purity 99.99% commercial alumina powder (Taimicron TM-DAR, Taimei Chemicals Co., Ltd., Tokyo, Japan, primary particle size 150 nm and specific surface area 13.7 $m^2\,g^{-1}$, the values determined by the producer from SEM micrographs and BET analysis, respectively) was used as a starting material. Doped powders (500 ppm of Mg, Y or Zr with respect to Al_2O_3) were prepared by mixing 100 g of the alumina powder with respective amounts of suitable precursors: $Mg(NO_3)_2{\cdot}6H_2O$ (p.a., Lachema Brno, Czech Republic), zirconium acetate, and $Y(NO_3)_3{\cdot}6H_2O$ (99.8% purity, Sigma Aldrich). The mixture was homogenized in a polyethylene jar in isopropanol (pure, Sigma Aldrich) with high purity alumina milling balls for 2 h. The water solution of ammonia was then added to precipitate respective hydroxides. The mixtures were then further homogenized for 2 h to complete the hydrolysis and the solvent was removed in vacuum evaporator. The powders were crushed with pestle in agate mortar, sieved through a 100 μm polyethylene sieve, calcined for 1 h at 800 °C in air, and sieved again to obtain a reasonably free flowing powder. The specimens containing MgO, Y_2O_3 and ZrO_2 are denoted respectively as AM, AY, and AZ. The reference alumina powder (denoted as A) was treated using the same procedure to ensure similarity with the doped powders.

In order to avoid calcination, which was found to impair densification behaviour of the used alumina powder,[24] an alternative way was used for preparation of MgO-containing mixtures. Doped powders were prepared by mixing the Taimicron TM DAR alumina powder with $MgAl_2O_4$ spinel (Baikalox Spinel S30CR, Baikowski, France, primary mean particle size 200 nm, specific surface area 30 $m^2\,g^{-1}$, the values determined by the producer by sedigraph test and BET analysis, respectively) in isopropanol for 24 h. The solvent was removed in vacuum evaporator and dried powder was sieved through a 100 and 40 μm polyethylene sieves. The powder prepared in this way is denoted as AMS. Untreated alumina powder (denoted as AA) was used as the reference sample.

The green bodies were prepared by uniaxial pressing of powders at 100 MPa with subsequent cold isostatic pressing at 250 MPa. The sintering experiments were carried out in an electrical furnace (NETZSCH GmbH, Selb, Germany) with $MoSi_2$ heating elements in air.

For the two-stage sintering regime the temperature T_1 was determined by heating the samples at 20 °C min^{-1} up to the maximum temperature in the interval between 1300 and 1475 °C, and then immediately cooled down to room temperature at the cooling rate 20 °C min^{-1}. During the two stage sintering the specimens were first heated to temperature T_1 without isothermal dwell, and subsequently cooled down to T_2 at a rate of 20 °C min^{-1}. The dwell time at the temperature T_2 (between 1150 and 1300 °C) ranged between 3 and 24 h. Finally, the specimens were cooled down to room temperature at 20 °C min^{-1}.

The density of sintered specimens was measured by mercury immersion, and expressed in per cent of the theoretical density of α-Al_2O_3 (3.98 g cm^{-3}). The microstructures were examined by scanning electron microscopy either on fracture surfaces (SEM; Tesla BS 300), or on polished and thermally etched cross sections (Zeiss, model EVO 40HV, Carl Zeiss SMT AG, Germany). The mean grain size was determined using the lineal intercept method on fracture surfaces.[25] Minimum of 200 grains was measured in order to obtain statistically robust set of data.

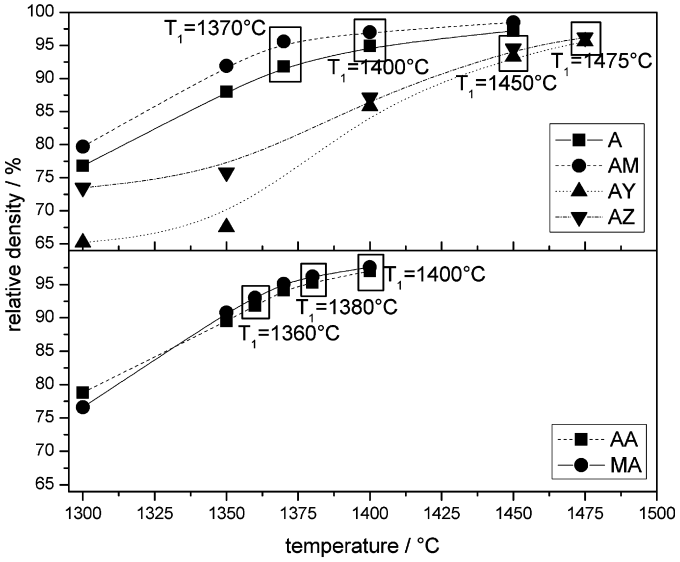

Fig. 1. The relative density–temperature dependences of alumina specimens sintered conventionally at the heating rate of 20 °C min^{-1} without isothermal dwell. (A) undoped and doped aluminas prepared from calcined powders and (B) untreated original powder AA and $MgAl_2O_4$-doped powder MA prepared without calcination. The temperatures T_1 selected for further experiments are highlighted by grey rectangles.

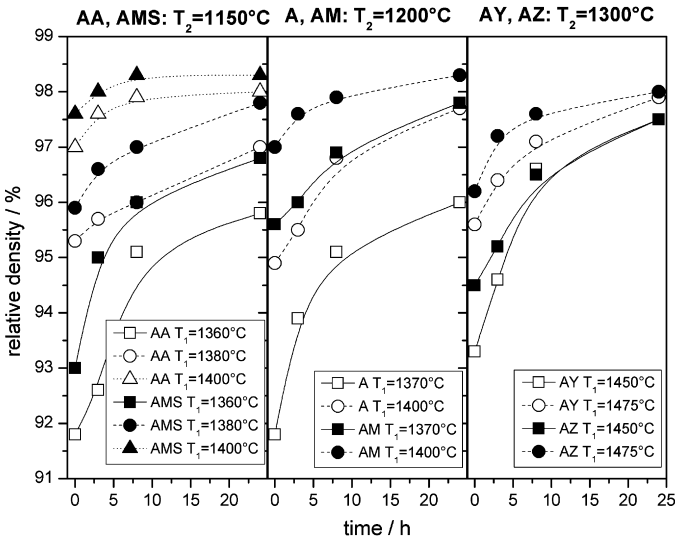

Fig. 2. Relative densities of prepared specimens as the function of the time of isothermal dwell at temperature T_2.

3. Results and discussion

According to Chen and Wang densification in the second, low-temperature step during the two-stage sintering is only possible if the pores in the first, high-temperature step achieve the dimensions under a critical threshold, where they become unstable against shrinkage.[1] Correct identification of the temperature T_1 is therefore prerequisite for achieving high density in the second step. Our previous results with the same alumina powder indicate that this state is achieved if the material densified to more than 92% of theoretical density, which roughly corresponds to the threshold of the final stage of sintering.[9] Fig. 1 summarises the relative densities of studied specimens heated to various temperatures without isothermal dwell. The influence of doping is quite obvious. The addition of MgO improved densification, whilst sintering of the alumina compacts is markedly impaired by the addition of zirconia and yttria, the latter being more efficient densification inhibitor, which is in agreement with previously published data.[15,21–23,26] The effect of doping is most pronounced at lower temperatures, and gradually disappears as the temperature nears 1475 °C.

Based on the results in Fig. 1 the temperatures T_1 were determined for the two-stage experiment, which ensured the relative density after the first step in the range between 91.8 and 97.6%. The temperature T_1 varied significantly for different compositions, e.g. 1360–1400 °C for undoped and MgO-doped materials, and 1450–1475 °C for Y_2O_3 and ZrO_2-doped specimens.

Each green body consolidation technique yields compacts with certain volume fraction and size of processing defects, which can be completely eliminated only under very harsh conditions, or cannot be eliminated at all. The presence of such defects is often the reason that the relative density of a piece of ceramic is not 100%, although normal densification is already completed. Specimens of all compositions were therefore sintered for 1 h at 1450 °C, which are the conditions exceeding those required for complete densification of the undoped powder (1 h at 1300–1350 °C as given by the producer). The maximum relative density did not in any case exceed 99%, which was thus considered the highest density that can be, under standard conditions, achieved for the specimens consolidated by axial and subsequent cold isostatic pressing. This value was therefore in further work considered as the highest relative density attainable by two-stage sintering.

In order to minimize the grain growth in the second step, the temperature T_2 was determined empirically as the lowest temperature at which the relative density close to 99% was achieved in less than 24 h of isothermal dwell. The relative densities after the two-stage sintering regime are summarised in Fig. 2.

For MgO doped (AMS) as well as undoped (AA) specimens prepared without calcination the temperature T_2 as low as 1150 °C was sufficient to achieve relative densities close to 99%. Calcination of the powder resulted in the increase of T_2 to 1200 °C and samples doped with Y_2O_3 and ZrO_2 required 1300 °C for near complete densification. The negative influence of calcination on sinterability of the powder could be explained by formation of aggregates, and overall decrease of surface activity of calcined powder.[24] The higher T_2 required for sintering of Y_2O_3 and ZrO_2 doped samples confirms densification retarding action of Y_2O_3 and ZrO_2 during two-stage sintering, comparable to that reported by other authors for conventional sintering.[27,28] The final density after the second step (apart from the T_2) was to large extent influenced by the relative density of the material after the first sintering step. Generally speaking, higher final density was achieved for the specimens whose density after the T_1 step was higher, but the relative change of density in the course of the T_2 isothermal dwell was smaller. The highest relative density achieved by the two-stage sintering was 98.3%, but based on

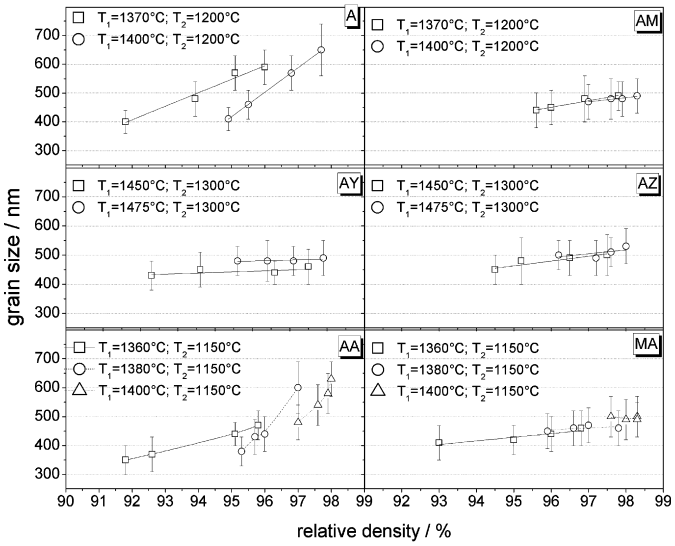

Fig. 3. Sintering trajectories of specimens densified with the use of two-stage regime.

the course of the density-time dependences in Fig. 2 further densification can be expected by extension of the isothermal dwell at T_2.

The main reason for application of two stage sintering is suppression of grain growth in the final stage sintering by application of the second, low temperature, heating step. A good graphic way for comparison of microstructure refinement is the grain size vs. relative density dependence called sintering trajectory. Fig. 3 summarises the sintering trajectories of studied samples. For undoped aluminas A and AA moderate grain growth of about 150–250 nm was observed, which represent 1.3–1.6 fold increase of the mean grain size in comparison to the grain size after completion of the first, high temperature, step. Doping led, in all cases, to suppression of grain growth in the final stage of densification, and to flat sintering trajectories. The suppression of the grain growth can be expressed by the relative increase of the mean grain size in comparison to the grain size after completion of the first stage. In nearly fully dense specimens after the second stage the mean grain size was only 1.02–1.12 fold higher, irrespective of the used dopant, which represents only negligible grain growth during the second step of sintering. In other words, whilst densification of undoped alumina by two-stage sintering was always accompanied by certain amount of grain growth,[5,9] small amount of dopants were able to suppress the grain growth in the final stage of sintering almost entirely. Interestingly, the effect was observed both for the grain growth accelerator (MgO), and inhibitors (Y_2O_3 and ZrO_2). The sintering trajectories of all doped specimens then fall essentially into one single line. The mean grain size of all doped dense samples was then about 500 nm. The value was independent both from the type of doping, and the powder pre-treatment. Nevertheless, doping with MgO, either in oxide or spinel form is considered as more advantageous in terms of lower sintering temperatures required to achieve high final density.

The mechanisms of action of the used dopants are likely not different for those described for conventional sintering. MgO addition was reported to result in transformation of interfaces from atomically smooth to atomically rough, with corresponding increase of surface and grain boundary diffusion, and increase of both densification and grain growth rate.[14] The promotion of densification by addition of magnesia in two-stage sintering is reflected by lower temperatures required to achieve high final density than in undoped or yttria and zirconia doped specimens, and the shift of the sintering trajectory to higher densities in comparison to undoped samples. The suppression of grain growth is explained by mutual impingement of growth by adjacent alumina grains.

The enhanced efficiency of two-stage sintering of Y and Zr-doped samples could be attributed to synergy effect of the two-stage sintering and the addition of grain growth inhibitors. This effect is usually attributed to segregation of dopant ions at alumina–alumina interfaces. There exist several mechanisms, which could efficiently suppress the grain growth. If the

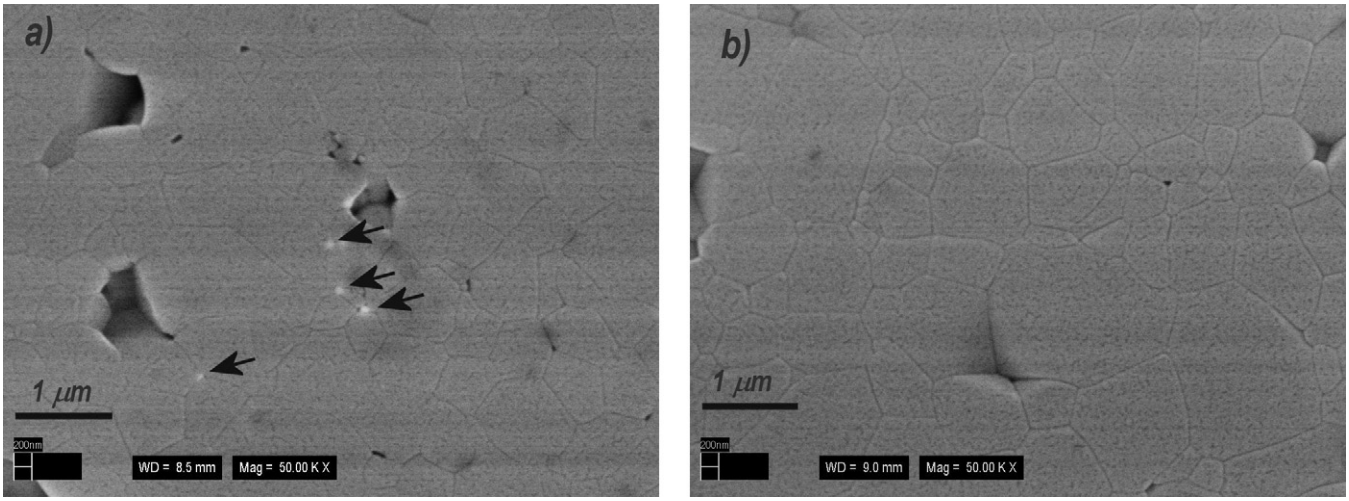

Fig. 4. Backscattered electron images of polished cross-sections of zirconia (a) and yttria (b) doped specimens sintered at 1450 °C for 1 h. The zirconia precipitates are marked with arrows.

concentration of dopants is sufficiently high, they precipitate in the form of discrete particles (such as ZrO_2), or react with the alumina matrix yielding another phase, such as yttrium–aluminium garnet (YAG) if Y_2O_3 is added.[29] In this case, the grain boundary mobility might be reduced by particle pinning. Backscattered electron images in Fig. 4 show the polished and thermally etched cross sections of Y_2O_3 and ZrO_2-doped specimens. No second phase precipitates were observed in yttria-doped samples. This is not surprising, as the precipitation of YAG in Y_2O_3-doped aluminas was found to be grain size dependent and no YAG precipitates were detected in alumina with grain size below 2 μm, and with the level of yttria comparable to that used in this work.[30] In sub-micron aluminas the yttria was found to be present almost entirely in the solute form.[29] A sporadic presence of ZrO_2 precipitates can be observed in Fig. 4a, the zirconia particles are marked by arrows. On the first sight, this observation contradict the literature data: no ZrO_2 precipitates were detected in the 1000-ppm-zirconium-doped Al_2O_3 ceramic with the mean grain size of 0.8 μm, and segregation of Zr^{4+} ions at the grain boundary was observed by STEM/EDS.[23,31] In this respect, small fraction of precipitated zirconia particles could indicate inhomogeneous distribution of the dopant in alumina matrix. However, the number of precipitates is too low to result in any observable pinning effect, which is known to be in alumina–zirconia composites active from 3 vol.% zirconia upwards.[32] Other mechanisms, resulting from atomic segregation of dopant ions at alumina interfaces are therefore likely responsible for the observed microstructure refinement. These include either the solute drag, or the increase of activation energy for surface diffusion and grain boundary mobility. Dopant segregation would also result in impaired densification, which is in accord with obtained data.

The influence of dopants on activation energies of densification and grain growth, and on the creation of "kinetic window" as proposed by Chen and Wang,[1] however, remains questionable, and requires further investigation.

4. Conclusions

Two-stage sintering experiments were carried out in order to evaluate the influence of the addition of 500 ppm of magnesia, zirconia and yttria to densification and grain growth of a sub-micron alumina powder. In undoped alumina microstructure coarsening was observed in the final stage of sintering, resulting in 1.6 fold increase of the mean grain size. Nearly dense undoped alumina with the mean grain size of 650 nm was prepared. Doping with Mg, Y, and Zr resulted in suppression of grain growth in the final stage of sintering. Doped samples were sintered to near full density with only 1.02–1.12 fold increase of the mean grains size. Doped MgO, ZrO_2 and Y_2O_3 materials with the mean grain size of 500 nm were prepared.

Acknowledgements

The financial support of this work by the grants VEGA 1/0603/09, VEGA 2/0036/10 and APVV 0485-09 is gratefully acknowledged. This publication was created in the frame of the project "Centre of excellence for ceramics, glass, and silicate materials" ITMS code 262 201 20056, based on the Operational Program Research and Development funded from the European Regional Development Fund.

References

1. Chen IW, Wang XH. Sintering dense nanocrystalline ceramics without final-stage grain growth. *Nature* 2000;**404**:168–71.
2. Wang XH, Deng XY, Bai HL, Zhou Z, Qu WG, Li LT, Chen IW. Two-step sintering of ceramics with constant grain-size II: $BaTiO_3$ and Ni–Cu–Zn ferrite. *J Am Ceram Soc* 2006;**89**:438–43.
3. Polotai A, Breece K, Dickey E, Randall C, Ragulya A. A novel approach to sintering nanocrystalline barium titanate ceramics. *J Am Ceram Soc* 2005;**88**:3008–12.
4. Binner J, Annapoorani K, Paul A, Santacruz I, Vaidhyanathan B. Dense nanostructured zirconia by two stage conventional/hybrid microwave sintering. *J Eur Ceram Soc* 2008;**28**:973–7.
5. Mazaheri M, Zahedi AM, Sadrnezhaad SK. Two-step sintering of nanocrystalline ZnO compacts: effect of temperature on densification and grain growth. *J Am Ceram Soc* 2008;**91**:56–63.
6. Huang YH, Jiang DL, Zhang JX, Linz QL. Fabrication of transparent lanthanum-doped yttria ceramics by combination of two-step sintering and vacuum sintering. *J Am Ceram Soc* 2009;**92**:2883–7.
7. Li D, Chen SO, Shao WQ, Wang DC, Li YH, Long YZ, Liu ZW, Ringer SP. Preparation of dense nanostructured titania ceramic using two step sintering. *Mater Technol* 2010;**25**:42–4.
8. Yang DY, Yoon DY, Kang SJL. Suppression of abnormal grain growth in WC–Co via two-step liquid phase sintering. *J Am Ceram Soc* 2011;**94**:1019–24.
9. Bodišová K, Šajgalík P, Galusek D, Švančárek P. Two-stage sintering of alumina with submicrometer grain size. *J Am Ceram Soc* 2007;**90**:330–2.
10. Hesabi ZR, Haghighatzadeh M, Mazaheri M, Galusek D, Sadrnezhaad SK. Suppression of grain growth in sub-micrometer alumina via two-step sintering method. *J Eur Ceram Soc* 2009;**29**:1371–7.
11. Maca K, Pouchly V, Zalud P. Two-step sintering of oxide ceramics with various crystal structures. *J Eur Ceram Soc* 2010;**30**:583–9.
12. Kanters J, Eisele U, Rödel J. Effect of initial grain size on sintering trajectories. *Acta Mater* 2000;**48**:1239–46.
13. Bennison SJ, Harmer MP. Effect of MgO solute on the kinetics of grain growth in Al_2O_3. *J Am Ceram Soc* 1983;**66**:C90–2.
14. Jo W, Kim DY, Hwang NM. Effect of interface structure on the microstructural evolution of ceramics. *J Am Ceram Soc* 2006;**89**:2369–80.
15. Berry KA, Harmer MP. Effect of MgO solute on microstructure development in $A1_2O_3$. *J Am Ceram Soc* 1986;**69**:143–9.
16. Long GG, Krueger S, Page RA. The effect of green density and the role of magnesium oxide additive on the densification of alumina measured by small-angle neutron scattering. *J Am Ceram Soc* 1991;**74**:1578–84.
17. McCune RC, Donlon WT, Ku RC. Yttrium segregation and YAG precipitation at surfaces of yttrium-doped α-Al_2O_3. *J Am Ceram Soc* 1986;**69**:C196–9.
18. Cawley JD, Halloran JW. Dopant distribution in nominally yttrium-doped sapphire. *J Am Ceram Soc* 1986;**69**:C195–6.
19. Cho JH, Harmer M, Chan P, Rickman HM, Thompson JMAM. Effect of yttrium and lanthanum on the tensile creep behavior of aluminum oxide. *J Am Ceram Soc* 1997;**80**:1013–7.
20. Cho J, Wang CM, Chan HM, Rickman JM, Harmer MP. Role of segregating dopants on the improved creep resistance of aluminum oxide. *Acta Mater* 1999;**47**:4197–207.
21. Fang J, Thompson AM, Harmer MP, Chan HM. Effect of yttrium and lanthanum on the final-stage sintering behavior of ultrahigh-purity alumina. *J Am Ceram Soc* 1997;**80**:2005–12.
22. Voytovych R, MacLaren I, Gülgün MA, Cannon RM, Rühle M. The effect of yttrium on densification and grain growth in α-alumina. *Acta Mater* 2002;**50**:3453–63.

23. Wakai F, Nagano T, Iga T. Hardening in creep of alumina by zirconium segregation at the grain boundary. *J Am Ceram Soc* 1997;**80**:2361–6.
24. Ghillányová K, Galusek D, Pentrák M, Madejová J, Bertóti I, Szepvölgyi J, Šajgalík P. The influence of ageing on consolidation and sinterability of a sub-micron alumina powder. *Powder Technol* 2011;**214**:313–21.
25. Nelson JA, Wurst JC. Lineal intercept technique for measuring grain size in two-phase polycrystalline ceramics. *J Am Ceram Soc* 1972;**55**:109.
26. Bae SI, Baik S. Critical concentration of MgO for the prevention of abnormal grain growth in alumina. *J Am Ceram Soc* 1994;**77**:2499–504.
27. Lartigue-Korinek S, Carry C, Priester L. Multiscale aspects of the influence of yttrium on microstructure, sintering and creep of alumina. *J Eur Ceram Soc* 2002;**22**:1525–41.
28. Loudjani MK, Cortés R. Study of the local environment around zirconium ions in polycrystalline α-alumina in relation with kinetic of grain growth and solute drag. *J Eur Ceram Soc* 2000;**20**:1483–91.
29. McCune RC, Donlon WT, Ku RC. Yttrium segregation and YAG precipitation at surfaces of yttrium-doped α-Alumina. *J Am Ceram Soc* 1986;**69**:C196–9.
30. Gruffel P, Carry C. Effect of grain size on yttrium grain boundary segregation in fine-grained alumina. *J Eur Ceram Soc* 1993;**11**:189–99.
31. Xue LA, Chen IW. Superplastic alumina at temperatures below 1300 °C using charge-compensating dopants. *J Am Ceram Soc* 1996;**79**:233–8.
32. Hirlinger MM, Lange FF. Hindrance of grain growth in Al_2O_3 by ZrO_2 inclusions. *J Am Ceram Soc* 1984;**67**:164–8.